Title

Experimental and modeling investigation of the effect of air preheat on the formation of NOx in an RQL combustor

Journal

Heat and Mass Transfer, 49(2)

ISSN

0947-7411

Authors

Samuelsen, GS
Brouwer, J
Vardakas, MA
et al.

Publication Date

2013-02-01

DOI

10.1007/s00231-012-1080-0

Heat Mass Transfer (2013) 49:219–231
DOI 10.1007/s00231-012-1080-0

ORIGINAL

Experimental and modeling investigation of the effect of air preheat on the formation of NO_x in an RQL combustor

G. S. Samuelsen · J. Brouwer · M. A. Vardakas · J. D. Holdeman

Received: 22 December 2011 / Accepted: 8 October 2012 / Published online: 25 October 2012

Abstract The Rich-burn/Quick–mix/Lean-burn (RQL) combustor concept has been proposed to minimize the formation of oxides of nitrogen (NO_x) in gas turbine systems. The success of this low-NO_x combustor strategy is dependent upon the links between the formation of NO_x, inlet air preheat temperature, and the mixing of the jet air and fuel-rich streams. Chemical equilibrium and kinetics modeling calculations and experiments were performed to further understand NO_x emissions in an RQL combustor. The results indicate that as the temperature at the inlet to the mixing zone increases (due to preheating and/or operating conditions) the fuel-rich zone equivalence ratio must be increased to achieve minimum NO_x formation in the primary zone of the combustor. The chemical kinetics model illustrates that there is sufficient residence time to produce NO_x at concentrations that agree well with the NO_x measurements. Air preheat was found to have very little effect on mixing, but preheating the air did increase NO_x emissions significantly. By understanding the mechanisms governing NO_x formation and the temperature dependence of key reactions in the RQL combustor, a strategy can be devised to further reduce NO_x emissions using the RQL concept.

G. S. Samuelsen · J. Brouwer · M. A. Vardakas
UCI Combustion Laboratory, University of California, Irvine, Irvine, CA 92697-3550, USA

Present Address:
M. A. Vardakas
Solar Turbines, San Diego, CA, USA

J. D. Holdeman (✉)
National Aeronautics and Space Administration, Cleveland, OH 44135, USA
e-mail: jjdholdeman@aol.com

List of symbols

A_J/A_M	Jet-to-mainstream area ratio $= (\pi d/2)^2/(H*S)$ $= n((d/2)/R)^2$ for a cylindrical duct
C	$(S/H)(J)^{0.5}$ for a rectangular duct $= \pi(2*J)^{0.5}/n$ for a cylindrical duct; derived in [13]
C_d	Orifice discharge coefficient
D	Round hole diameter
d_j	Effective round hole diameter $= (d)(C_d)^{0.5}$
DR	Jet-to-mainstream density ratio, ρ_J/ρ_M
H	Duct height for a rectangular duct $= R$ for a cylindrical duct
J	Jet-to-mainstream momentum-flux ratio $= (\rho V^2)_{jets}/(\rho U^2)_{main}$ $= (MR)^2/DR/(C_d)^2/(A_J/A_M)^2$
MR	Jet-to-mainstream mass-flow ratio $= (\rho VA_{total})_{jets}/(\rho UA_{can\ cross\text{-}section})_{main}$ $= (DR)(V_J/U_M)(C_d)(A_J/A_M)$
n	Number of round holes in quick-mix module
R	Radius of the quick-mix module
r	Radial distance from the module center
S	Orifice spacing
U	Axial velocity
U_M	Unmixed mainstream velocity
V_J	Jet exit velocity
x	Downstream distance; x = 0 at orifice leading edge
ρ_J	Density of jet flow
ρ_M	Density of mainstream flow
ϕ	Equivalence ratio $= (\text{fuel/air})_{\text{actual}}/(\text{fuel/air})_{\text{stoichiometric}}$

1 Introduction

The Rich-burn/Quick-mix/Lean-burn (RQL) combustor concept was introduced in 1980 by Mosier et al. [1] as a strategy to reduce oxides of nitrogen (NO_x) emissions from stationary gas turbine engines using fuels that were high in fuel-bound nitrogen. Later in the 1980′s, studies co-sponsored by the National Aeronautics and Space Administration (NASA) and the Environmental Protection Agency (EPA), continued [2–5] that were motivated by the RQL's potential for having low NO_x emissions for these fuels. A study of the effect on NO_x emissions from fuels having high amounts of fuel-bound nitrogen was reported by Mao and Barth [6] in a staged combustor using CH_3NH_2 doping to simulate fuel-bound nitrogen.

In the 1990′s the RQL concept was selected by the High Speed Research (HSR) program at NASA as a candidate for the reduction of oxides of nitrogen in engines for a High Speed Civil Transport (HSCT) [7–11] in part because in aeroengine applications an RQL may be preferred over lean premixed prevaporized (LPP) options due to safety considerations and overall performance (e.g. stability) of the RQL throughout the duty cycle. Today, RQL technology is used in aeroengines deployed commercially.

In stationary applications, lean premixed combustor technology is the standard. Safety considerations are not as severe, the duty cycle is more constrained, and the reduction in NO_x emissions is more substantial for LPP combustors in contrast to RQL technology. However, RQL combustor technology is of growing interest for stationary applications due to the attributes of more effectively processing fuels of complex and varying composition. The latter is becoming more important with the increasing international competition for fuels in general, and an increasing interest in liquefied natural gas, biomass fuels, and "opportunity fuels" (e.g., land-fill gases, digester gases, well-head gases) to either complement domestic fuel sources or serve as the sole source to a large region of a country (e.g. Southern California) or a country as a whole (e.g. South Korea).

1.1 RQL concept

The RQL (Fig. 1) is based on the premise that the primary zone of a gas turbine combustor operates most effectively with rich mixture ratios in the primary zone. A "rich-burn" condition ($\phi > 1$; see Fig. 2) in the primary zone (1) enhances the stability of the combustion reaction by producing and sustaining a high concentration of energetic hydrogen and hydrocarbon radical species, and (2) minimizes the production of nitrogen oxides due to the relatively low temperatures and low population of oxygen containing intermediate species. The effluent exiting from a rich primary zone will be high in the concentration of hydrogen (H_2), carbon monoxide (CO), and partially oxidized and partially pyrolyzed hydrocarbon species (HC). As a result, the effluent will contain both a substantial fuel value and pollutant composition, and cannot be exhausted without further processing.

The addition of oxygen in the mixing zone quickly converts the non-oxygen containing species in the Total Fixed Nitrogen (TFN) in the rich zone effluent to NO_x [6], but is needed to oxidize the high concentrations of carbon monoxide, hydrogen, and hydrocarbon intermediates. If no additional NO_x is formed in the mixing and lean zones, the NO_x concentration at the combustor exit would be approximately equal to the sum of the mole fractions of the prompt-NO and the major non-oxygen containing species in the rich zone effluent times the rich-to-total mass-flow ratio. Thus, the goal in achieving low NO_x in an RQL combustor is to mix air into the rich zone effluent quickly and in such a manner as to minimize the formation of thermal-NO_x to achieve an exhaust at the exit of the combustor that is comprised of the major products of combustion (CO_2, H_2O, N_2, O_2) and a near-zero concentration of pollutants (e.g., NO_x, CO, HC).

The mixing of the injected air takes the reaction through the conditions most vulnerable for the high production of oxides of nitrogen (see Fig. 2). Because the challenge is to rapidly mix air ($\phi = 0$) into the rich effluent ($\phi > 1$) to quickly create a lean composition ($\phi < 1$), the moniker "Quick-mix" is adopted to emphasize this requirement. A major candidate is a row of jets in crossflow (as shown schematically in Fig. 3) which has been found to provide rapid mixing.

1.2 Jet mixing

To address the conditions particular to applications of jets in crossflow (JIC), numerous studies have been conducted

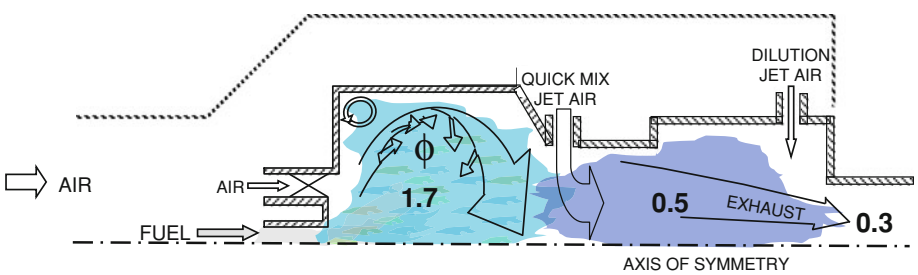

Fig. 1 Rich-Burn/Quick-Mix/Lean-burn combustor ϕ, equivalence ratio)

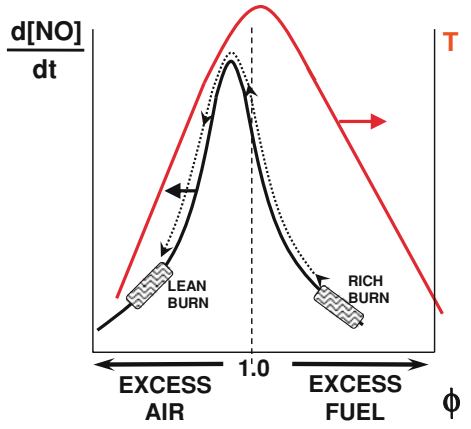

Fig. 2 RQL strategy

Fig. 3 Schmetic of laboratory model combustor

to yield insight on jet structure and penetration, jet entrainment of crossflow fluid, and the flow field distributions resulting from jet mixing [12–20]. These studies have investigated single unbounded jets, both bounded and unbounded multiple jets, asymmetrically bounded jets, heated jets, a heated mainflow, reacting flows, or the doping of either the jets or mainflow with a tracer to allow the measurement of scalars in the flow downstream of the jet orifices. While a variety of jet orifice shapes have been studied (e.g., triangular, tear-drop, square, rectangular, bluff, slanted, and streamlined slots), no option has been identified that penetrates significantly farther or mixes faster than a round jet in an unbounded crossflow.

For a confined flow, as in a gas turbine combustor, design methods for both rectangular and cylindrical configurations have been identified at Cranfield and NASA. These are described by Lefebvre [21].

1.2.1 Non-reacting JIC mixing

Historically, an early correlation (circa 1960) for the maximum penetration of multiple jets injected normal to a crossflow was developed by Norster and is given by Eqs. (4–20) in [21]:

$$Y_{max} = 1.25(d_j)(J)^{0.5}/(1+MR) \quad (1)$$

In an RQL mixing section, the *MR* is much higher ($\sim 10\times$) than in the dilution zone of a conventional combustor. Since the density ratio *DR* ($= \rho_J/\rho_M$) and momentum-flux ratio *J* ($= (\rho_J V_J^2)/(\rho_M U_M^2)$) are about the same for the two applications, the biggest difference between the jets in conventional and RQL combustors is orifice size.

While the cylindrical geometry has been extensively researched and is directly relevant to combustor can configurations, modern large annular combustor configurations have spawned investigations of jets in crossflow in rectangular geometries.

Insight on scalar distributions resulting from mixing of confined jets in crossflow stemmed from the studies conducted in the 1970's and 1980's to address the mixing behavior associated with dilution jets in conventional gas turbine combustors. The extensive non-reacting studies of rows of jets in crossflow in rectangular, annular, and cylindrical ducts that are summarized in Holdeman [14] were funded by NASA to evaluate geometrical features (e.g., orifice spacing, opposed rows of orifices, axial staging of orifices, orifice shape, flow area convergence, effects of flow-area curvature, and a non-uniform mainstream scalar) and operating conditions (e.g. density ratio, momentum-flux ratio, mass-flow ratio) with the goal to optimize the mixing in a gas turbine combustor. Later, the NASA JIC empirical model from [14] (without the curvature effects) was implemented in the Excel® spreadsheet reported in [15–18].

For rectangular, annular, or cylindrical ducts the jet spacing *S/H* was observed to be inversely proportion to the square root of the momentum-flux ratio *J* such that:

$$C = (S/H)(J)^{0.5} \quad (2)$$

For **one-side injection** optimum jet penetration was observed when C was ~ 2.5; significant underpenetration was observed for C less than half of the optimum value; significant overpenetration was observed when C was more than double the optimum value. For **opposed rows**, corresponding C values are $\sim$half these (i.e. $C_{optimum} \sim 1.25$; for significant underpenetration C is <0.63; for significant overpenetration C is over 2.5). For a rectangular or annular duct the jets can be injected from one side, or there can be opposed rows of aligned or staggered jets. For multiple jets in a cylindrical duct, injection is always one sided and the duct height [e.g. *H* in Eq. (2)] is the radius of the can.

If one assumes that the orifice spacing given by Eq. (2) should be applied to a can at the radius that divides the cylindrical cross section into equal area cylindrical and annular sections, one can derive a relation for the optimum number of holes in a cylindrical duct from Eq. (2) [14]. For $C = 2.5$:

$$n = \pi(2J)^{0.5}/2.5 \quad (3)$$

Traditionally, studies such as Hatch et al. [22] have defined "optimal mixing" as the shortest distance downstream from

the jet orifice needed to obtain a uniform profile for key scalars (e.g., temperature, species concentration). The hypothesis is that the optimal mixing defined in this manner will minimize the production of oxides of nitrogen. Due to the complex set of variables, a design of experiments statistical approach was used by Kroll et al. [23] to select optimum variables from among the multiple factors that can affect jet mixing. In addition to non-reacting experiments and use of design of experiments methods, empirical modeling and CFD have been effectively employed both independent of and in conjunction with experiments.

The studies NASA funded in the 1990's focused on optimizing the mixing section in the Rich burn/Quick mix/Lean burn (RQL) combustor scheme in rectangular, annular, and cylindrical ducts for both non-reacting and reacting flows [19, 20]. These papers included design procedures for achieving the most rapid mixing for both cylindrical [19] and rectangular ducts [20].

1.2.2 Reacting JIC mixing

Reacting flow studies of jets in a crossflow have been conducted in both conventional and RQL combustor configurations to complement the non-reacting studies and assess the impact of heat release on the mixing processes [24–29].

For the RQL-motivated studies at atmospheric pressure by Leong et al. [28, 29], a mixture of propane and air was employed to generate a representative rich-burn effluent, and a specially designed "conditioning" section was used to create a uniform presentation (e.g., temperature, velocity, composition, and concentration) of the rich effluent to the Quick-mix section. The injection of the jet air into the rich effluent results in a combination of mixing and reaction between the rich-burn effluent and the jet air (Fig. 3). Measurements of temperature, species composition, and species concentration can then be made downstream of the jet orifices in order to establish the efficacy of mixing as a function of downstream distance.

The results from the reacting experiments reveal that distributions of a conserved scalar from non-reacting experiments generally provide a satisfactory description of the mixing of a conserved scalar for reacting jets in a crossflow. Overall, the jets in a cylindrical duct need to penetrate to approximately half of the can radius in order to maximize the mixing and avoid either under-penetration or over-penetration.

The studies by Leong et al. [28, 29] reported results for reacting flow experiments in a cylindrical duct at atmospheric pressure without inlet air preheat. A carbon balance technique similar to that of Jones et al. [30] was used by Leong et al. [28, 29] to obtain the equivalence ratio. Alternate methods for obtaining the local equivalence ratio in a reacting flow were investigated by Demayo et al. [31].

The first exploration of the relation between mixing and NO_x emissions in an RQL-motivated study utilized the results of non-reacting experiments, and superimposed analytically the kinetics of NO_x production [32]. The results suggested that the best mixer might not minimize NO_x emissions.

Experimental measurements under reacting conditions at elevated pressure were provided by Meisl et al. [33]. The inlet air was preheated but the temperature was not varied, nor were the number of orifices in the mixing section varied. The study focused on the effect of varying pressure on NO_x emissions. The authors of [33] noted the two well-known sources for the emissions of NO_x, namely prompt- and thermal-NO_x. The first of these is the formation of NO in the fuel-rich primary zone [34], a contribution that Meisl et al. [33] found was relatively insensitive to pressure. The second source is the formation of thermal NO_x that may occur in the Quick-mix section which increases significantly with pressure. The study by Meisl et al. [33] also concluded that NO_x emissions are minimized by optimal mixing.

A study by Vardakas et al. [35] extended the work reported by Leong et al. [28, 29] to address the effects on both mixing and emissions of varying inlet air preheat and varying the number of orifices. This study investigated configurations with 8, 12, 14, and 22 round holes at $J = 57$ to give over- to optimum to under-penetrating jets. The experiments were conducted at atmospheric pressure with the jet and main air preheated independently. Selected experimental results from Vardakas et al. [35] were published in Holdeman et al. [36].

The primary conclusion based on the experimental results was that mainstream air preheat increases NO_x more that jet air preheat, and that an "optimum" mixer may not minimize NO_x emissions.

2 Experiment

2.1 Facility

The experimental facility used in this study consisted of a premixing zone, a fuel-rich combustion zone, and a jet-mixing section as shown in Fig. 4. In the premixing zone, propane gas was mixed with air upstream of the ignition point. Fuel-rich combustion was stabilized downstream of the quarl by a swirl-induced recirculation zone. To dissipate the swirl in the flow and to introduce a uniform non-swirling flow into the mixing section, the fuel-rich product was passed through an oxide-bonded silicon carbide

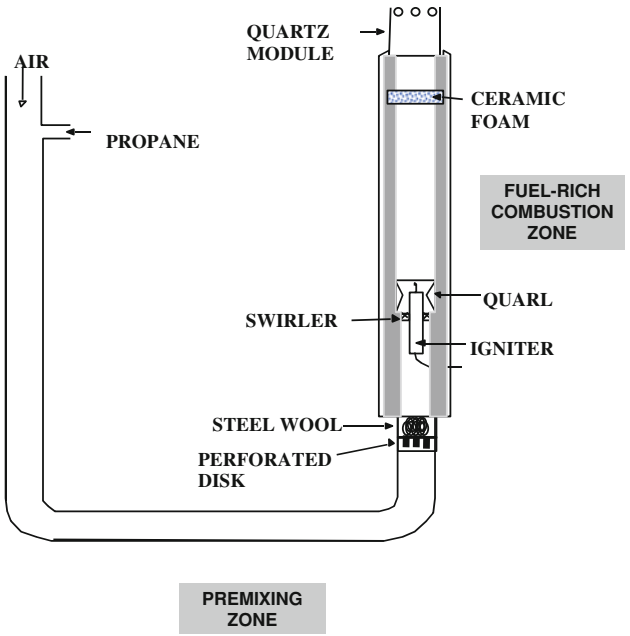

Fig. 4 Schematic of experimental rich product generator with quartz RQL module

(OBSiC) ceramic foam matrix (Hi-Tech Ceramics) with a rated porosity of 10 pores/in.

The mixing section was modular and included a cylindrical section through which the mainstream effluent passed, and to which jet air was supplied from a surrounding plenum. The plenum for the jet air was fed by four equally-spaced air ports located toward the base of the plenum. A high-temperature steel flow-straightening device installed in the plenum conditioned and equally distributed the jet air entering the mixing module.

The mixing modules were 280 mm (11 in.) in length with inner and outer diameters of 80 mm (3.15 in.) and 85 mm (3.35 in.). The row of orifices was positioned with its centerline 115 mm (4.5 in.) downstream from the module entrance. An alumina-silica blend of ceramic fiber paper provided sealing between the module and the stainless steel mating surfaces to form the plenum for the air jets.

Recirculating heaters of 20 and 25 kW were utilized to supply the necessary preheat to the main and jet air lines respectively. The preheat temperatures were independently established and controlled.

2.2 Measurements

For each module, species concentration measurements were obtained in a two-jet sector for a plane at $x/R = 1$ (plane 5 in Fig. 5a) where x/R was measured from the leading edge of the mixing module orifices. Note that x/d = R/d for the data reported herein because $x = R$.

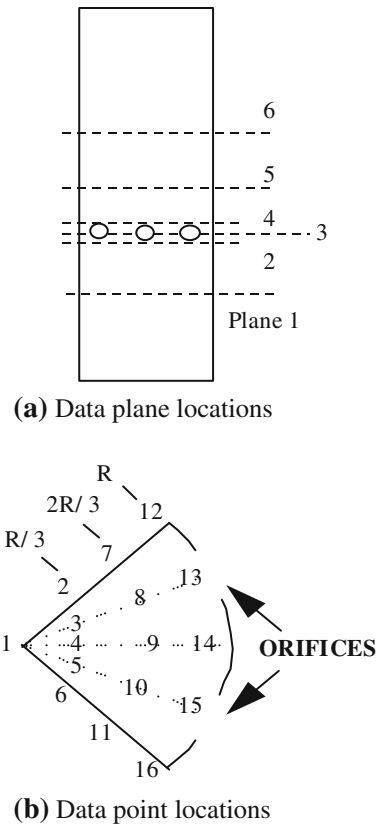

(a) Data plane locations

(b) Data point locations

Fig. 5 Measurement locations

Each planar grid consisted of 16 points spread over a sector that included two orifices (Fig. 5b). The points included one point located at the center of the duct, and five points along each of the arcs at $r/R = 1/3$, 2/3, and 1.

The measurement points along each arc were distributed such that two points were aligned with the center of the orifices and three were aligned with the midpoint between orifice centers for all cases.

Species concentration measurements were obtained by sampling through a water-cooled stainless-steel probe by routing the sample through a heated line connected to the emission analyzers. Water was condensed from the gas before the sample was analyzed by non-dispersed infrared (NDIR) analysis for CO and CO_2, paramagnetic analysis for O_2, flame ionization detection (FID) for total hydrocarbons, and chemiluminesence (CLD) for NO_x. Data are reported as measured and were not "corrected" for either the ambient humidity or the expected water content of the flow.

The extractive emissions measurement protocol was conventional. The analyzers were standardized equipment which was checked frequently with span gases. As for the relation between what exists in the flow and what is measured; this is a classical question, and they are assumed to be the same when standard procedures are followed.

2.3 Probe design

A double-jacked water-cooled stainless steel probe 762 mm (30 in.) in length was used to extract gas samples from the quick mixing section (Fig. 6). The probe measured 8 mm in outer diameter and tapered to 3.2 mm at the tip. A 45 degree bend was made 25.4 mm (1 in.) from the tip. The probe design was influenced by the research in [23] that reported that a thermocouple probe with a 45-degree angled tip was best as it biased the mainstream and jet flows equally in the orifice region. The probe location was fixed and the rig was traversed to obtain the measurements. The plane of the angled probe tip was positioned such that the tip was pointed toward the center of the sector wall.

2.4 Measurement uncertainty

A measure of the uncertainty of the data is given by analyzing the species measurements to determine the midplane and centerplane means and variances [36]. In a perfect world, the 3 midplane measurements would be equal and the 2 centerplane measurements would be equal at a given radius, but they often aren't. Their variability is a measure of both spatial and species uncertainty in the measurements. This is discussed further in [36].

2.5 Experimental conditions

The experiments were performed for a jet-to-mainstream momentum-flux ratio (J) of 57 and a mass-flow ratio (MR) of 2.5. The total effective area of the mixing module orifices is 9 cm^2 (1.4 $in.^2$). The ratio of the total effective jet area to the cross-sectional area of the duct is 0.18. The fuel-rich equivalence ratio and overall equivalence ratio are 1.66, and 0.45, respectively. The operating pressure for the system is one atmosphere.

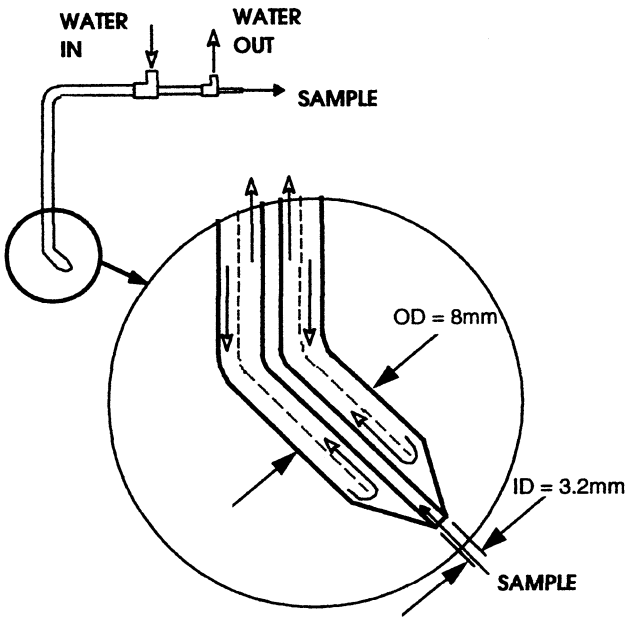

Fig. 6 Probe design

Table 1 Operating conditions

Parameter	Value
Momentum–flux ratio, J	57
Mass-flow ratio, MR	2.5
Discharge coefficient, C_d	0.72
(Total jet area)/(cross-sectional area of duct), A_J/A_M	0.25
Non-preheated inlet air temperature	22 °C (72 °F)
Inlet preheat temperature	260 °C (500 °F)

The experimental results presented show comparisons between non-preheated air and preheated jet and main air cases. Inlet temperatures and other operating conditions for the experiment are noted in Table 1.

3 Analysis

These analyses supplement the experimental results reported in [35, 36] with chemical equilibrium and chemical kinetics calculations to gain insight into the formation of NO_x in the rich [34], mixing, and lean (called the 2nd stage in [6]) stages.

The NASA Equilibrium Code [37] was used to perform chemical equilibrium calculations with the thermodynamic data base of Kee et al. [38]. The modeling assumptions made were for fixed equivalence ratios and constant enthalpy.

Chemical kinetic calculations were performed using the SENKIN computer code, and the CHEMKIN III Subroutines [39, 40]. The chemical kinetic mechanism of Miller and Bowman [41] was used to describe the lower hydrocarbon combustion and NO_x formation chemical kinetics along with the propane oxidation mechanism of Sundaram and Froment [42]. The conditions of the model represented those of the experiment (e.g. temperature and stoichiometry in each zone) except that the model did not account for any effects due to mixing and dispersion.

4 Results and discussion

NO_x data were obtained to investigate the effect of preheating jet and main air flows in the RQL combustor. Data for the 12 round-hole quick-mixing module are presented here as in [35, 36] for conditions without preheat and with

both main and jet air preheated to the same temperature. Chemical equilibrium and kinetic modeling calculations were performed to gain insight into the NO_x formation mechanisms governing the experiments and to compare calculated levels to measured NO_x concentrations.

4.1 Chemical equilibrium

Chemical equilibrium results are presented in Fig. 7, illustrating the dominant fixed nitrogen species participating in NO_x formation, destruction, and emission mechanisms in the RQL combustor. Note that nitric oxide (NO) dominates the equilibrium species that are present for most of the equivalence ratios presented ($0.4 < \phi < 1.66$). Ammonia (NH_3) and hydrogen cyanide (HCN) are increasingly important only in the fuel-rich regime ($\phi > 1$) while nitric oxide (NO), nitrogen dioxide (NO_2), and nitrous oxide (N_2O) are the major fixed nitrogen species for fuel-lean conditions ($\phi < 1$). An important feature in these results is the existence of a minimum for total fixed nitrogen (TFN) species. The equivalence ratio corresponding to this minimum for the non-preheat air case is approximately 1.66, the operating fuel-rich zone equivalence ratio used in the experiment. As the inlet air temperature increases, however, the condition of minimum TFN shifts to higher equivalence ratios (more fuel-rich conditions) as shown in Fig. 8.

Mao and Barth [6] reported that the minimum in TFN shifted to larger rich zone ϕ's and higher NO concentrations as the loading of CH_3NH_2 in the feed increased. As there is no fuel-bound nitrogen in the fuel used in our study, we would expect to have rich zone minimums in both the ϕ for the TFN minimum and the NO concentration there.

Figure 9 shows rich zone experimental data for the non-preheated air and 500 °F (533 K) preheated air cases. For the 500 °F case, the minimum TFN corresponds to $\phi = 2.0$ with a higher equilibrium TFN at $\phi = 1.66$ (approximately 8 ppm versus 2 ppm). The experimental NO_x data at the exit of the fuel-rich zone in the RQL combustor in Fig. 9 illustrates the effect of preheated main air on NO_x in the fuel-rich zone, and is consistent with the equilibrium results of Fig. 8. Thus, one would expect increased NO_x emissions in the preheat case simply because one was no longer operating the fuel-rich zone at the optimal stoichiometry to minimize TFN for preheated air conditions.

4.2 Chemical kinetics

The equivalence ratios used for the chemical kinetic modeling correspond to operating equivalence ratios for

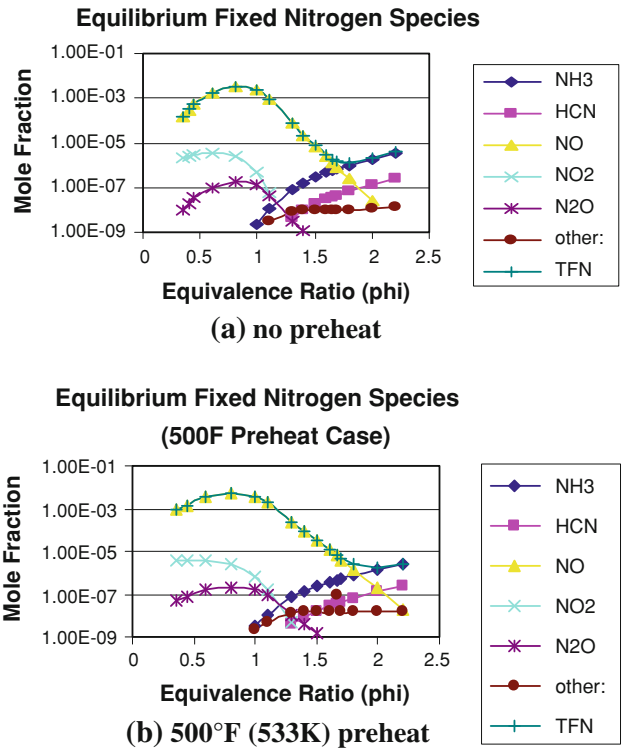

Fig. 7 Chemical equilibrium fixed nitrogen species results for the non-preheat and 500 °F (533 K) preheat cases

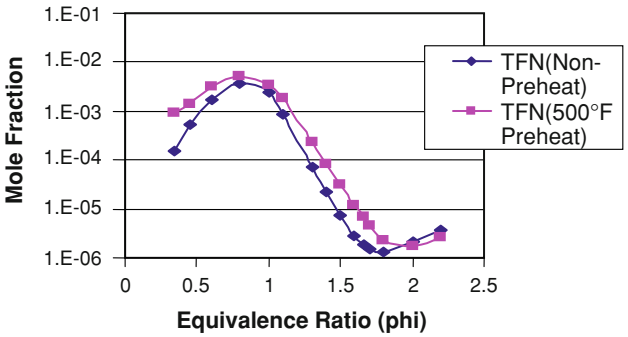

Fig. 8 Total fixed nitrogen comparison between non-preheat and preheat conditions

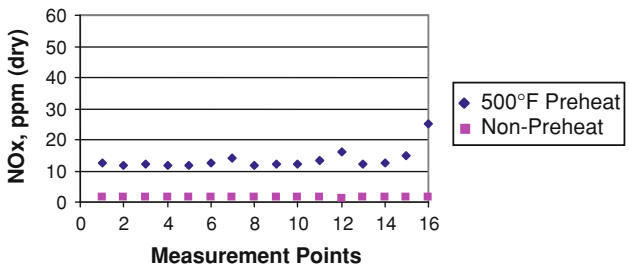

Fig. 9 NO_x Measurements in RQL fuel-rich zone (x/R = −1) for preheat and non-preheat conditions

the fuel-rich ($\phi > 1$) and fuel-lean ($\phi <$!) zones of the RQL combustor. Chemical kinetic calculations were also performed for stoichiometric ($\phi = 1$) conditions because of their importance to NO_x formation in transitioning from fuel-rich to fuel-lean zones of the combustor which occurs in the quick-mix zone. The adiabatic flame temperature was used as a baseline case for each of the chemical kinetic simulations. In addition, two lower temperatures were simulated to account for various levels of heat loss that might occur in practical systems. Measurements of temperature that were made in the RQL combustor were consistently bounded by the chemical kinetic modeling conditions.

4.2.1 $\phi = 1.66$ (Fuel-rich zone results)

The chemical kinetic results for the fuel-rich conditions of $\phi = 1.66$ are presented in Fig. 10 for constant temperature conditions of 2,000, 1,573, and 1,425 K. The major fixed nitrogen species identified by the model are nitric oxide (NO), hydrogen cyanide (HCN) and ammonia (NH_3) which is consistent with the chemical equilibrium results of Fig. 4. In all cases (adiabatic or with heat-loss) the NO and HCN kinetics are quite rapid leading to near equilibrium concentrations in less than 2 ms. The ammonia concentration continually increases with time and temperature in the range investigated.

4.2.2 $\phi = 1.00$ (Stoichiometric results)

As air is introduced to the fuel-rich zone effluent in the quick-mix section of the RQL combustor there is a transition in overall equivalence ratio from rich ($\phi > 1$) to lean ($\phi < 1$). This transition does not occur instantaneously, but rather is characterized by finite mixing times resulting in spatial and temporal inhomogeneities and fluctuations between these two stoichiometries. During this mixing process stoichiometric or near-stoichiometric conditions and high temperatures can exist locally with a corresponding increase in potential for the formation of NO_x and other fixed nitrogen species.

Figure 11 shows chemical kinetics calculations for stoichiometric conditions. As in the previous case adiabatic conditions are shown (2,364 K here) and the other two temperatures represent levels of heat loss which bound temperatures measured in the experiment in the quick-mix zone. Note that the adiabatic temperature for stoichiometric conditions is higher than that for rich conditions.

In Fig. 11, the rate of NO production under stoichiometric conditions is shown to be exceedingly fast. The other fixed nitrogen species which are significant for these conditions include nitrous oxide (N_2O) and nitrogen dioxide (NO_2), both with significantly lower concentrations compared to

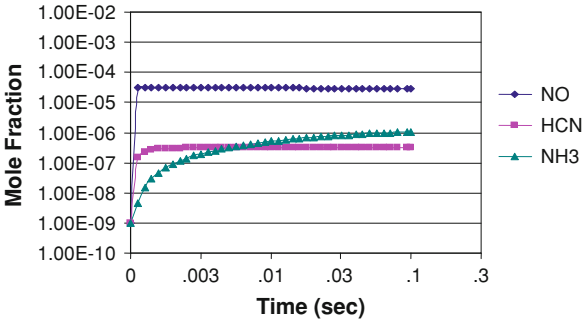

(a) Temperature = 2000 K, ϕ = 1.66

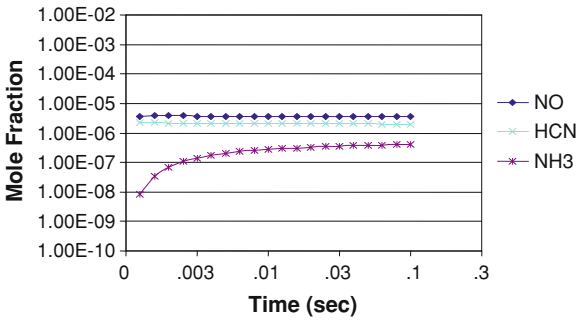

(b) Temperature = 1573K, ϕ = 1.66

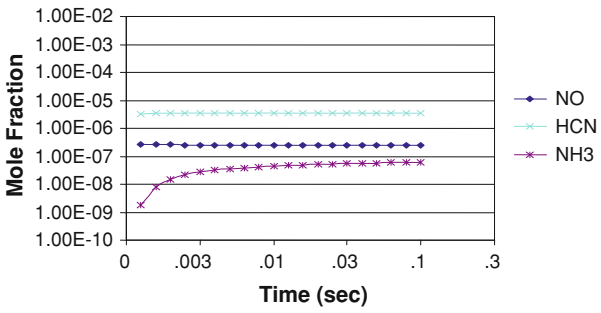

(c) Temperature = 1425 K, ϕ = 1.66

Fig. 10 Chemical kinetic evolution of primary fixed nitrogen species for $\phi = 1.66$ conditions similar to RQL fuel-rich zone

NO. NO forms very rapidly for all temperature conditions investigated. As with the rich conditions in Fig. 10, NO concentration levels for stoichiometric conditions shown in Fig. 11 are very dependent on temperature with mole fractions of over 1E − 03 (1,000 ppm) for the 2,364 K case, less than 1E − 03 (1,000 ppm) for the 2,215 K case, and approximately 1E − 04 (100 ppm) for the 2,103 K case, all obtained within 2 ms. The N_2O and NO_2 species are produced almost as quickly as the NO, but stay consistently below a mole fraction of 1E − 06 (1 ppm). The NO results show that the concentration level in stoichiometric regions can range from a mole fraction of 1E − 03 (1,000 ppm) to 1E − 04 (100 ppm) depending on temperature.

Although the thermal-NO_x mechanism can produce substantial NO_x in the quick-mix zone, the objective is to

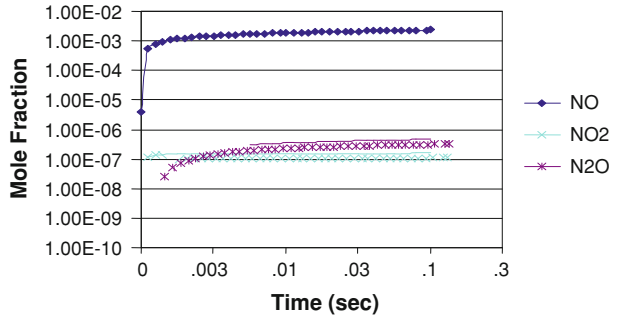

(a) Temperature = 2364 K, ϕ = 1.00

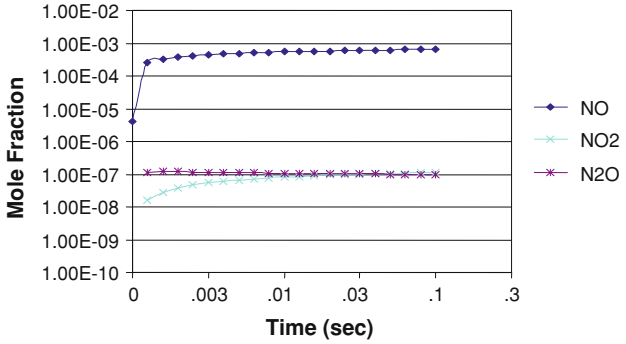

(b) Temperature = 2215 K, ϕ = 1.00

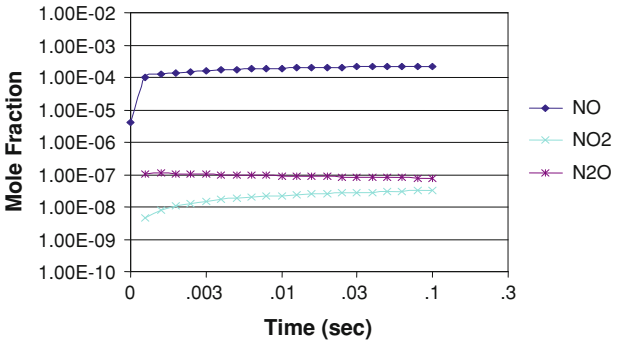

(c) Temperature = 2103 K, ϕ = 1.00

Fig. 11 Chemical kinetic evolution of primary fixed nitrogen species for $\phi = 1.00$

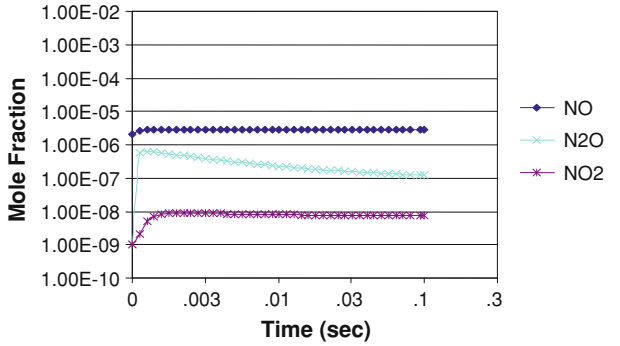

(a) Temperature = 1600K, ϕ = 0.45

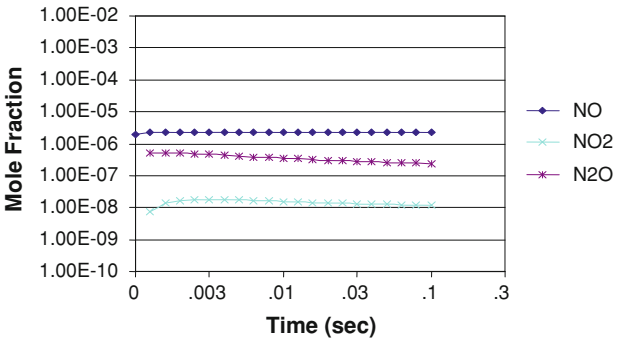

(b) Temperature = 1450 K, ϕ = 0.45

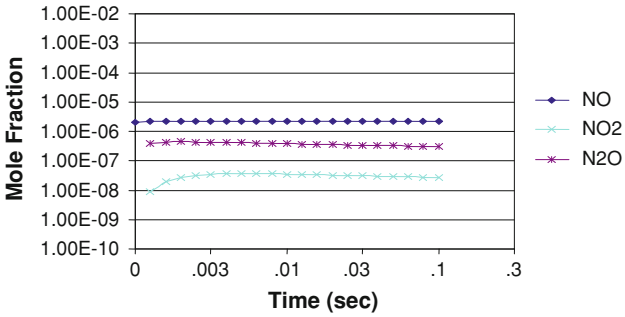

(c) Temp = 1350K, ϕ = 0.45

Fig. 12 Chemical kinetic evolution of primary fixed nitrogen species for $\phi = 0.45$. Conditions similar to conditions in the fuel-lean zone

minimize it so the combustor NO_x emissions are dominated by contributions from the prompt-NO_x and fuel-NO_x mechanisms.

4.2.3 $\phi = 0.45$ (Fuel-lean zone results)

Chemical kinetic calculations representing the fuel-lean zone of the RQL combustor are presented in Fig. 12. The simulation was performed by addition of sufficient air to the products of the fuel-rich zone ($\phi = 1.66$) to create the $\phi = 0.45$ conditions. Although the formation of NO is rapid for these conditions, the NO concentrations that are observed are significantly lower than those observed for either the stoichiometric or fuel-rich conditions. This is due to the lower temperatures of the fuel-lean zone (the excess air dilutes the mixture and lowers the temperature). The results of Fig. 12 indicate that most of the NO_x is not formed in the fully mixed fuel-lean zone of the combustor since single digit levels are all that are produced for $\phi = 0.45$ even with a long residence time.

4.3 Experimental results

Experimental data from Vardakas et al. [35] are shown in parts (a) and (b) of Fig. 13 for the non-preheat and main & jet preheat cases using the 12-hole module. The data shown in Fig. 13 indicate a significant increase in NO_x for the preheated case. A comparison of the various modules

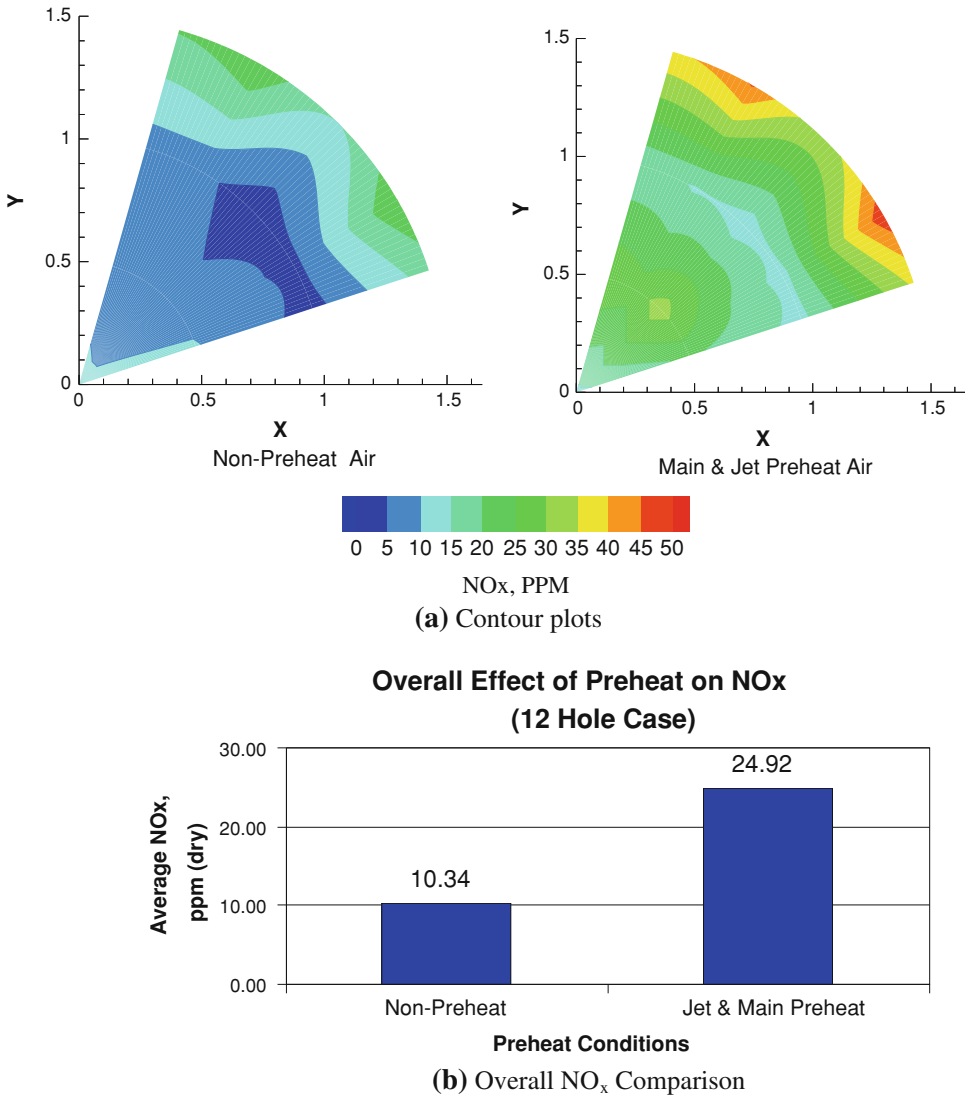

Fig. 13 Experimental NO_x data at x/R = 1 and J = 57 for the 12 hole module for non-preheat and jet and main air preheat conditions

(a) Contour plots

(b) Overall NO_x Comparison

(8-, 12-, 14-, and 22-round-hole) for all preheat conditions is presented in Vardakas et al. [35].

Figure 13(a) presents contour plots of the NO_x distribution for conditions without preheat and with both streams preheated. These plots show the effect that jet penetration has on determining the locations of peak NO_x concentration. The contour plots indicate that concentrations are high in the shear layers on both sides on the maximum jet penetration but the highest NO_x concentrations occur near the wall of the module in the wakes of the jets.

The effect of main & jet air preheat on overall NO_x emissions is presented in the bar chart in Fig. 13b and shows a large increase in overall NO_x emissions with both streams preheated. The results of Vardakas et al. [35] showed a significantly larger increase in NO_x emissions with both streams preheated than there was with no preheat and when only the jet air was preheated.

The variations of the averages for the cases shown vary from a low of $\sim$10 ppm for the case without preheat to a high of $\sim$25 ppm with both streams preheated.

NO_x can be produced by several mechanisms (prompt-, fuel-, and thermal-NO_x mechanisms), but when thermal NO_x formation is minimized, the NO_x is being produced primarily in the fuel-rich zone, and through conversion from other TFN species in the early mixing stage. The fuel-NO_x mechanism can convert the fuel-rich zone total fixed nitrogen (TFN) species other than NO (e.g., NH_3, HCN), which are the primary non-oxygen containing nitrogen species in the fuel-rich zone, to NO_x with relatively high conversion [6]. Although the chemical modeling does not take into account the effects of the mixing jets, the modeling results suggest that most of the NO_x observed in the experimental data is formed either in the quick-mix zone or in the fuel-rich zone.

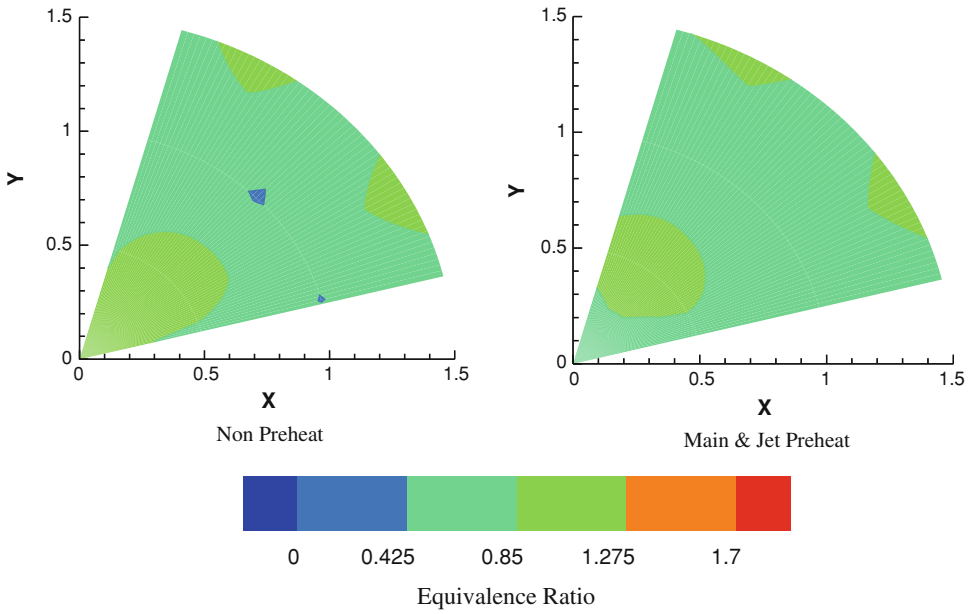

Fig. 14 Jet Equivalence Ratio Distribution Plots at x/R = 1 and J = 57 for the 12 round-hole module for non-preheat and jet & main air preheat conditions. The fuel-rich equivalence ratio and overall equivalence ratio are 1.66, and 0.45, respectively

This information can be used to devise technique(s) to further reduce overall NO_x formation in the RQL combustor. With preheat NO_x formation in the fuel-rich zone is higher than optimal because the optimal stoichiometry for minimum TFN shifts to more fuel-rich conditions as temperatures increase. Temperature based control of the fuel-rich zone stoichiometry is suggested.

The increased dependence of overall NO_x emissions on main air preheat suggests another optimization of the RQL concept. NO_x could be reduced by increasing heat transfer from the fuel-rich zone to the fuel-lean zone. One strategy could be to pass the jet air through the fuel-rich zone combustor liner to transfer heat from this zone to the quick-mix and fuel-lean zones which do not have as significant a dependence upon preheat temperature.

The distributions of equivalence ratios at x/R = 1 and J = 57 for the 12-hole module are given in Fig. 14. Preheat has almost no effect on jet penetration and mixing as expected, and the equivalence ratio distributions are quite uniform since the 12 hole configuration is a nearly optimum mixer at J = 57. As in Leong et al. [28, 29] the distributions in these plots were determined by noting that carbon atoms in carbon containing species are conserved [30].

Note that the completely mixed condition for a conserved scalar at $MR = 2.5$ would be $\phi = 0.45$. Unmixed mainstream fluid would be $\phi = 1.66$ and unmixed jet fluid would be $\phi = 0$.

5 Summary and conclusions

An experiment was performed to expand upon earlier work by incorporating preheated inlet air, and examining the effect it has on NO_x production. To further understand the mechanisms involved, chemical equilibrium and kinetic modeling was done. The following was revealed in this study:

- An important feature in these results is the existence of a minimum for total fixed nitrogen (TFN) species.
- Nitric oxide (NO) dominates the TFN species that are present for most equivalence ratios from $\phi = 0.4$ to $\phi = 1.66$.
- Ammonia (NH_3) and hydrogen cyanide (HCN) are increasingly important only in the fuel-rich regime.
- Under air preheat conditions, the fuel-rich zone should be operated at a higher equivalence ratio to reduce TFN production in this zone.
- NO_x is formed in less than 2 ms at all conditions.
- There exists sufficient residence time for significant amounts of NO to be formed in each zone.
- An optimization of the RQL concept could include increases in the heat transfer from the fuel-rich zone to the mixing and fuel-lean zones and temperature-based control of fuel-rich zone stoichiometry.

These conclusions are based upon chemical equilibrium, chemical kinetics, and experimental results that point to primary production of NO_x in the fuel-rich and early mixing zones. The mechanisms that lead to this NO_x production and emissions are prompt-NO_x and fuel-NO_x. Thermal-NO_x formed in the mixing zone can dominate emissions so NO_x formation via this mechanism must be minimized in an RQL combustor.

Acknowledgments The experimental work was supported by cooperation agreement NCC 3-412 from the NASA Glenn Research Center and the complementary chemical equilibrium and kinetics calculations were funded by the UCI Combustion Laboratory

(UCICL) at the University of California, Irvine. The authors would also like to thank the Combustion Branch at the NASA Glenn Research Center for providing for the Open Access publication and color printing of this paper.

References

1. Mosier SA, Pierce RM (1980) Advanced combustor systems for stationary gas turbine engines, phase I. Review and preliminary evaluation, vol I, contract 68-02-2136, FR-11405, Final Report, U.S. Environmental Protection Agency, March
2. Novick AS, Troth DL (1981) Low NO_X heavy fuel combustor concept program, NASA CR-165367 (same as DOE/NASA/0148-1), October
3. Lew HG, Carl DB, Vermes, G, DeZubay EA, Schwab JA, Prothroe D (1981) Low NO_X heavy fuel combustor concept program–phase 1: combustion technology generation, NASA CR-165482 (same as DOE/NASA/0146-1), October
4. Beal G, Hinton B, Kemp F, Russel P, Sederquist R (1981) Low NO_X heavy fuel combustor concept program, NASA CR-165512 (same as DOE/NASA/0149-3), October
5. Kemp FS, Sederquist RA, Rosfjord TJ (1982) Low NO_X heavy fuel combustor concept program–phase 1A: coal gas addendum final report, NASA CR-165577 (same as DOE/NASA/0149-) January
6. Mao F, Barat RB (1996) Minimization of NO during staged combustion of CH_3NH_2. Combust Flame 105(4):557–568
7. Shaw RJ, Gilkey S, Himes R (1993) Engine technology challenges for a 21st century high-speed civil transport, NASA TM-106216, September
8. Rosfjord TJ, Pagent FC (2001) Experimental assessment of the emissions control potential of a rich/quench/lean combustor for high speed civil transport aircraft engines, NASA CR—2001-210613, January
9. Holdeman JD, Chang CT, Nguyen HL (2001) Low Emissions RQL Flametube combustor component test results, NASA/TM—2001-210678, January
10. Chang CT, Holdeman JD, Nguyen HL (2001) Low Emissions RQL flametube combustor test results, NASA/TM–2001-211107, July
11. Peterson CO, Sowa WA, Samuelsen GS (2002) Performance of a model rich burn-quick mix-lean burn combustor at elevated temperature and pressure, NASA/CR-2002-211992, December
12. Margason RJ (1993) Fifty years of jet in cross flow research, presented at computational and experimental assessment of jets in cross flow, AGARD Conf Proc 534, April
13. Demuren AO (1994) Modeling jets in cross flow. NASA contractor report 194965, August (same as ICASE Report No. 94-71, August 1994)
14. Holdeman JD (1993) Mixing of multiple jets with a confined subsonic crossflow. Prog Energy Combust Sci 19:31–70. doi: 10.1016/0360-1285(93)90021-6 (similar to AIAA Paper 91-2458 and NASA TM 104412, June 1991)
15. Holdeman JD, Smith TD, Clisset JR, Lear WE (2005) A spreadsheet for the mixing of a row of jets with a confined crossflow. NASA/TM—2005-213137, February
16. Holdeman JD, Clisset JR, Moder JP, Lear WE (2006) On the mixing of single and opposed rows of jets with a confined crossflow. NASA/TM—2006-214226, October
17. Holdeman JD, Clisset JR, Moder JP (2010) Spreadsheet calculations for jets in crossflow: opposed rows of inline and staggered holes and single and opposed rows with alternating hole sizes. NASA/TM—2010-216100, July (an excerpt was published in Heat and Mass Transfer, 48(2):412–424 (Feb 2012), doi: 10.1007/s00231-011-0913-6 and another excerpt was published in the J Eng Gas Turbines Power 132(June 2010):64502-1-7
18. Holdeman JD, Clisset JR, Moder JP (2011) Spreadsheet calculations for jets in crossflow: opposed rows of slots slanted at 45°. NASA/TM—2011-215980, December
19. Holdeman JD, Liscinsky DS, Oechsle VL, Samuelsen GS, Smith CE (1997) Mixing of multiple jets with a confined subsonic crossflow: part I—cylindrical ducts. J Eng Gas Turbines Power 119(10):852–862. doi:10.1115/1.2817065 (same as ASME Paper 96-GT-482 and NASA TM 107185, June 1996)
20. Holdeman JD, Liscinsky DS, Bain DB (1999) Mixing of multiple jets with a confined crossflow: part II–opposed rows of orifices in rectangular ducts. J Eng Gas Turbines Power 121(7):551–562. doi:10.1115/1.2818508 (same as ASME Paper 97-GT-439 and NASA TM 107461, June 1997)
21. Lefebvre AH (1999) Gas turbine combustion, 2nd edn. Taylor and Francis, New York
22. Hatch MS, Sowa WA, Samuelsen GS, Holdeman JD (1995) Jet mixing into a heated cross flow in a cylindrical duct: influence of geometry and flow variations. J Propuls and Power 11(3):393–400 (same as AIAA-92-0773 and NASA TM 105390, Jan. 1992; derived from NASA CR-194473, June 1996)
23. Kroll JT, Sowa WA, Samuelsen GS, Holdeman JD (2000) Optimization of orifice geometry for cross flow mixing in a cylindrical duct. J Propuls Power 16(6):929–936 (same as AIAA-94-0219 and NASA TM 106436, Jan. 1994; derived from NASA CR-198482, April 1996)
24. Noyce JR, Sheppard CGW, Yamba FD (1981) Measurements of mixing and species concentration within a gas turbine type combustor. Combust Sci Technol 25:209–217
25. Heitor MV, Whitelaw JH (1986) Velocity, temperature, and species characteristics of the flow in a gas-turbine combustor. Combust Flame 64:1–32
26. Richards CD, Samuelsen GS (1990) The role of primary jet injection on mixing in gas turbine combustors. Twenty-Third Symp (Int) Combust 23:1071–1077
27. Bicen AF, Tse DGN, Whitelaw JH (1990) Combustion characteristics of a model can-type combustors. Combust Flame 80:111–125
28. Leong MY, Samuelsen GS, Holdeman JD (1999) Mixing of jet air with a fuel-rich, reacting crossflow. J Propuls Power 15(5):617–622 (same as WSS/CI Paper No. 97S-034 and NASA TM 107430, Apr. 1997; derived from NASA CR-195375, Sept. 1996)
29. Leong MY, Samuelsen GS, Holdeman JD (2000) Optimization of jet mixing into a rich, reacting crossflow. J Propuls Power 16(5):729–735 (also AIAA-98-0156 and NASA/TM–97-206294, Dec. 1997; see also NASA CR-195375, Sept. 1996)
30. Jones WP, McDonell V, McGuirk JJ, Milosavljevic VD, Taylor AMKP, Whitelaw JH (1993) The calculation of mean mixture fractions in turbulent non-premixed methane flames from aspiration-probe measurements. Department of Mechanical Engineering, Imperial College of Science, Technology, and Medicine, Report TFS/93/13, March
31. Demayo TN, Leong MY, Samuelsen GS, Holdeman, JD (2003) Assessing jet-induced spatial mixing in a rich, reacting crossflow. J Propuls Power 19(1):14–21 (same as NASA/CR—2004-212886, Jan. 2004)
32. Hatch MS, Sowa WA, Samuelsen GS, Holdeman JD (1992) Influence of geometry and flow variation on the NO formation in the quick mixer of a staged combustor. Accepted for publication

in the J Eng Gas Turbines Power but distribution was initially restricted by HSR (same as NASA TM–105639, December 1995; derived from NASA CR-194473, June 1996)
33. Meisl J, Koch R, Kneer R, Wittig S (1994) Study of NO_x emission characteristics in pressurized staged combustor concepts. Twenty-Fifth Sym (Int) Combust 25:1043–1049
34. Fenimore CP (1976) Reactions of fuel-nitrogen in rich flame gases. Combust Flame 26:249–256
35. Vardakas MA, Leong MY, Brouwer J, Samuelsen GS, Holdeman JD (1999) The effect of air preheat at atmospheric pressure on the formation of NO_x in the quick-mix sections of an axially staged combustor. NASA TM-1999-209431, August
36. Holdeman JD, Vardakas MA, Chang CT (2008) Mixing of multiple jets with a confined subsonic crossflow: part III—the effects of air preheat and number of orifices on flow and emissions in an RQL mixing section. NASA/TM–2008-215151, March (similar to J Fluids Eng 129(11):1460–1467)
37. Gordon S, McBride BJ (1976) Computer program for calculation of complex chemical equilibrium composition, rocket performance, incident and reflected shocks, and Chapman-Jouquet Detonations. NASA SP-273, Interim Revision
38. Kee RJ, Rupley FM, Miller JA (1990) The chemkin thermodynamic data base. Sandia National Laboratories report, SAND87-8215, Sandia Natioinal Laboratories, Albuquerque, NM
39. Lutz AE, Kee RJ, Miller JA (1987) SENKIN: a FORTRAN program for predicting homogeneous gas phase chemical kinetics with sensitivity analysis, Sandia report SAND87-8248-UC401, Combustion research facility, Sandia Natioinal Laboratories, Albuquerque, NM, July
40. Kee RJ, Rupley FM, Meeks E, Miller JA (1996) CHEMLIN III: a FORTRAN chemical kinetics package for the analysis of gas phase chemical and plasma kinetics, Sandia report, SAND96-8216-UC405. Sandia National Laboratories, Albuquerque, NM
41. Miller JA, Bowman CT (1989) Mechanism and modeling of nitrogen chemistry in combustion. Prog Energy Combust Sci 15:287–338
42. Sundaram KM, Froment GF (1979) Kinetic of coke deposition in the thermal cracking of propane. Chem Eng Sci 34:635